2012

Mini Vapour Cycle System For High Density Electronic Cooling Applications

Simone Mancin
simone.mancin@unipd.it

Claudio Zilio

Luisa Rossetto

Mini Vapour Cycle System For High Density Electronic Cooling Applications

Simone MANCIN[1]*, Claudio ZILIO[1], Luisa ROSSETTO[1]

[1*]Università di Padova, Dipartimento di Ingegneria Industriale,
Via Venezia 1, 35131, Padova, Italy
Ph. +39 049 8276882, Fax +39 049 8276896
claudio.zilio@unipd.it, luisa.rossetto@unipd.it

* Corresponding Author
@-mail: simone.mancin@unipd.it

ABSTRACT

This paper reports the preliminary experimental results of a mini Vapour Cycle System (VCS) for electronic thermal management applications. The water cooled miniature scale refrigeration system uses R134a as working fluid and implements a new concept oil-free linear compressor prototype. In the range of operating test conditions investigated, the cooling capacity of the system varied from 46 to 310 W while the coefficient of performance (*COP*) ranged between 1.05 and 5.54. Particular attention was dedicated to the cold plate design, which had to meet the requirements established by the aeronautical standards. The cold plate was equipped with 15 thermocouples in order to analyze the wall temperatures distribution. The suitability and feasibility of the proposed cold plate for electronic thermal management in aeronautical environment is critically discussed, basing on the experimental results.

1. INTRODUCTION

In the recent years, the aeronautical industry has been moving towards a More Electrical Aircraft (MEA) concept (i.e. use of a single optimized electrical system instead of separately optimized and traditional electric, hydraulic and pneumatic sub-systems) for the design of new commercial aircrafts, with the primary aim of reducing fuel burn. The European Commission co-funded since year 2000 several research projects following the roadmap outlined in the Strategic Research Agenda of the Vision 2020 for Aeronautics. The new design strategy of electrical and power electronics systems for aeronautical applications brings about the need of remarkable changes in dissipated power management. The field experience gathered in the last decades by the avionics suppliers companies have demonstrated that one of the most critical challenges is linked to the thermal management of electronics: the aeronautical environment is characterized by harsh ambient conditions and by severe volume and mass constraints for the electronic packaging. Considering the aeronautical application, according to ARINC 600 specification (2006) an electronic packaging consists of multiple line replaceable units (LRUs) (electronic modules) inserted in a rack assembly. Each electronic equipment with its cooling system must comply with the design requirements reported in the ARINC 600 specification (2006).

As the number of electrical and electronic systems increases, their physical sizes decrease, and the spacing between electrical components decreases, both the total amount of heat generated (and thus which needs to be dissipated) and the power density (the heat generated per unit volume) increases significantly. The current state-of-the-art in heat transfer according to ARINC 600 is air-cooling: it is a general agreement in the scientific community that current air-cooling technologies are asymptotically approaching their limits imposed by available cooling area, available air flow rate, fan power and noise (Wei et al., 2007, Webb, 2007, Kandlikar and Grande, 2004).

Consequently, the thermal management architecture of aeronautical electronic packaging needs to be significantly stretched to meet these challenges (www.primae.org). One of the options could be the integration of a miniature vapor cycle system (VCS), thus allowing the thermal management of the electronic equipment using the high –efficient two-phase heat transfer process during vaporization inside a “cold plate” and the heat rejection at a temperature level higher than the ambient one through the refrigerant condensation.

A thorough review of miniature VCS applications has been presented recently by Barbosa et al. (2012). None of the works available in the open literature refers to aeronautical electronic packaging thermal management with VCS.
The challenging target of integrating a mini-VCS inside an ARINC package requires a throughout optimization of the heat exchangers design.
This paper presents the experimental measurements of a mini-VCS equipped with a cold plate specifically designed for aeronautical electronic thermal management applications, which operates with an oil-free compressor prototype. The heat is rejected to the ambient by means of water cooled condenser. The cold plate was designed to be implemented in aeronautical packaging where each heat sink has to maximize its compactness, weightlessness, reliability and efficiency.

2. EXPERIMENTAL APPARATUS

A reference miniature refrigeration system consists of four main components: a compressor, a condenser, a throttling device and an evaporator, also named cold plate. Figure 1 shows a schematic of the test rig including also the locations of the measurement devices. As it can be noted, additional components have been implemented in the test rig to allow the correct operation of the mini-VCS and also to permit the analysis of the system performance. In particular, a liquid separator has been inserted at the outlet of the cold plate in order to protect the compressor from any possible liquid flow in the suction line.

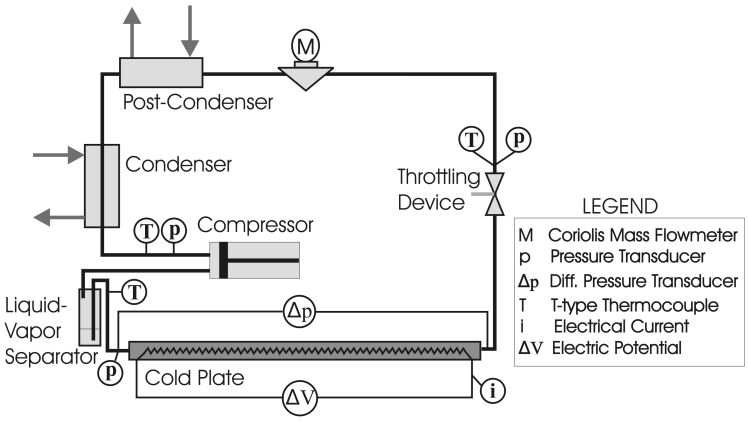

Figure 1: Schematic of the mini-VCS set up.

In the liquid separator, a T-type (Copper-Constantan) thermocouple is inserted to measure the refrigerant temperature at the outlet of the evaporator. The condenser is split in two water cooled heat exchangers, which condense and subcool the superheated gas. The condensers are two tube-in-tube heat exchangers each fed by two independent water flow rates controlled by two thermostatic baths allowing to set different water temperatures and thus, to control the subcooling temperature at the outlet of the second heat exchanger in order to set the desired operating test conditions at the inlet of the cold plate.
Then the subcooled liquid reaches the Coriolis effect flowmeter, which measures its mass flow rate with an accuracy of ±0.1% of the reading; after that, a needle micro-metering valve is used as the throttling device. Particular attention has been devoted to the cold plate design, which must comply the volume constraints specified by the aeronautical standards. As shown in fig. 2, the cold plate has been obtained from copper plate of sizes: 400 mm long, 20 mm wide and 10 mm thick. Three guides have been milled on the top side of the copper plate where a 2 mm ID tube has been brazed for a total length of 1.2 m; on the bottom side, other two guides have been machined to hold a Ni-Cr resistance wire, which simulates the heat load being powered by a stabilized DC power supply. In the lateral sides of the copper plate, fifteen holes have been drilled to locate as many T-type thermocouples with a pitch of 25 mm. The holes are 10 mm deep: eight holes have been obtained on one side and seven on the other. As the outcome, it is possible to measure the temperature with a pitch of 25 mm along an ideal line in the center of the cold plate rectangular cross section, from the refrigerant inlet side to the refrigerant outlet side. The electrical power is indirectly measured by means of a calibrated reference resistance (shunt) and by the measurement of the effective EDP (Electrical Potential Difference) of the resistance wire inserted in the cold plate. Accuracy of the electrical power supplied to the sample is within ±0.13% of the measured value. The pressure is measured in three different locations: two absolute pressure

transducers with an accuracy of ±130 Pa are positioned in the suction and discharge lines while the third one with an accuracy of ±400 Pa, is located before the throttling device. An additional differential pressure transducer with an accuracy of ±25 Pa is used to measure the refrigerant pressure drop during the vaporization process in the cold plate. As described, all the temperatures are measured by means of calibrated T-type thermocouples with an accuracy of ±0.05 K; in particular, the refrigerant temperature is measured in the liquid-vapor separator, at the outlet of the compressor, and at the inlet of the throttling device in an adiabatic mixing chamber.
The compressor is a prototype oil-free unit, which operates at constant speed; the cooling capacity is controlled by varying the displacement of the compressor. The development of this unit is presented elsewhere in the same conference (Ribeiro, 2012).

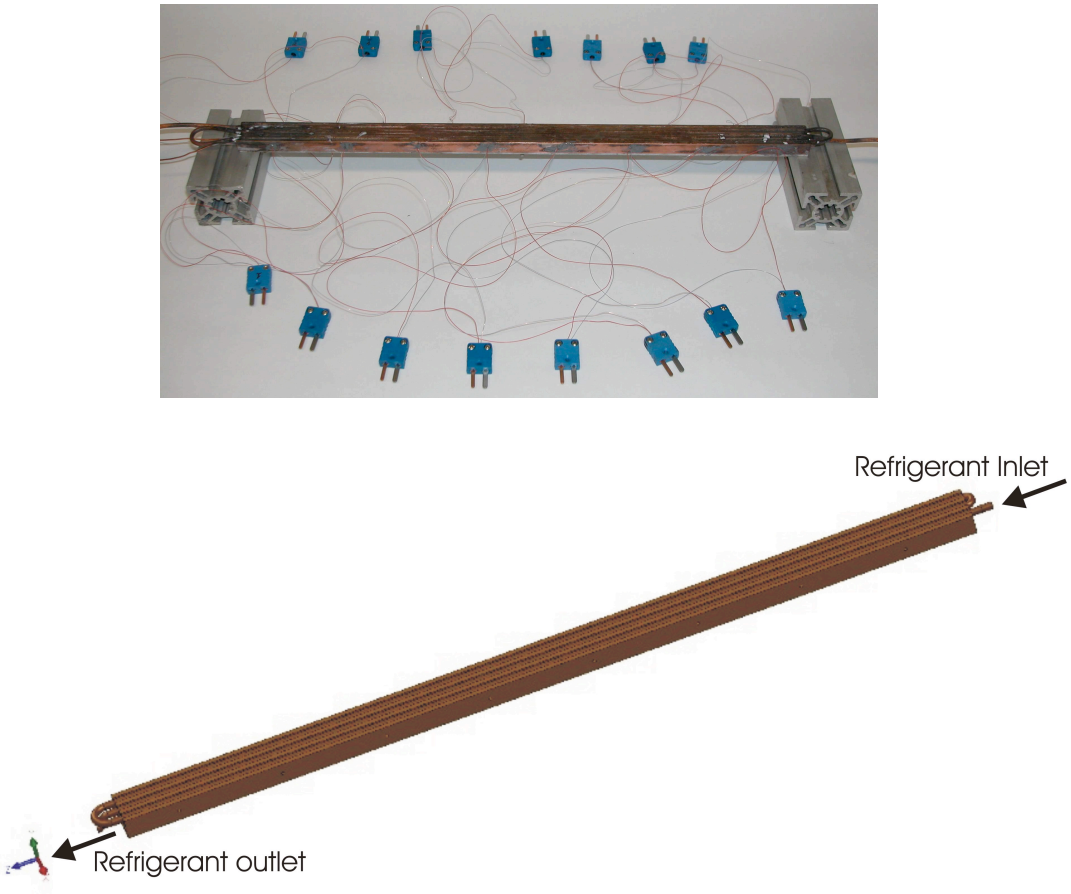

Figure 2: A photo (Top) and a drawing (Bottom) of cold plate.

4. MINI-VCS PERFORMANCE

The tests have been run at constant refrigerant suction pressure of around 0.49 MPa, i.e. by keeping constant the saturation temperature at around 15 °C at the outlet of the cold plate. Four different condensing levels have been investigated by adjusting the water temperatures of the secondary loops: 30 °C, 40 °C, 50 °C, and 60 °C. By means of an electronic driver, it is possible to set piston displacement.
The measurements were taken during steady state conditions by imposing the necessary heat flux, which led to a maximum wall temperature of 70 °C. By adjusting the needle micro-metering valve it was possible to set the desired evaporation temperature. The procedure implied that the electrical power was tuned till the maximum temperature was reached and then, the measurement was recorded as the average value of 50 readings.
The mini-VCS performance is presented in terms of electric power rejected by the cold plate (P_{EL}) (that is, within a maximum 4% misbalance, the VCS cooling capacity) and coefficient of performance (*COP*) which is defined as the ratio between the electrical power dissipated by the cold plate (P_{EL}) and the power adsorbed by the compressor (P_{comp}), as:

$$COP = \frac{P_{EL}}{P_{comp}} \tag{1}$$

These two parameters are plotted against the pressure ratio between the compressor discharge (p_{dis}) and suction (p_{suc}) pressure values, as:

$$p_R = \frac{p_{dis}}{p_{suc}} \tag{2}$$

Figure 3 reports the coefficient of performance (*COP*, eq. 1) plotted against the pressure ratio (p_R, eq. 2) as a function of the set piston displacement, which has been varied from 25 to 90%. Keeping constant the suction pressure, the different pressure ratios refer to the investigated condensation levels; in particular, setting the condensation temperature from 30 to 60 °C, the pressure ratio varies from 1.60 to 3.35. As expected, the highest values of *COP* are exploited at the lowest pressure ratio of 1.60 and the performance decreases as the pressure ratio increases. The piston displacement slightly affects the refrigeration system performance especially at low pressure ratio; as the pressure ratio increases, the effects of the piston displacement become somehow more noticeable.

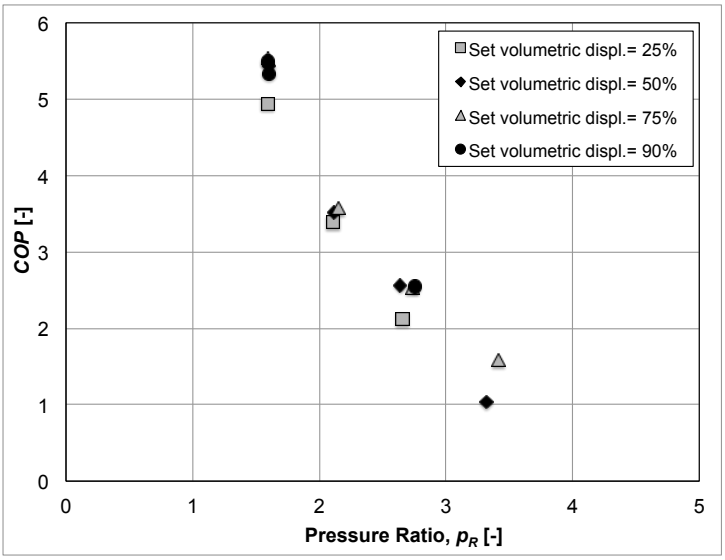

Figure 3: Coefficient of Performance (*COP*) plotted against the pressure ratio as a function of the piston displacement. Data collected at constant suction pressure of 0.49 MPa (T_{sat}=15 °C).

Figure 4 reports the cooling capacity plotted against the set piston displacement as a function of the condensation temperature; it clearly appears that the heat dissipated by the cold plate increases as the piston displacement increases. Furthermore, at constant piston displacement, the cooling capacity increases when decreasing condensation temperature; for instance, at the 50% of the maximum displacement, the heat rejected passes from 50 W at 60 °C of condensation temperature to 240 W at Tc=30 °C.

5. COLD PLATE ANALYSIS

Figure 5 and 6 show the experimental values of the cold plate refrigerant pressure drop and inlet vapor quality plotted against the piston displacement as a function of the condensation temperature. As expected, the pressure drops increase with the set piston displacement and when decreasing the condensation temperature because of the increasing on the refrigerant mass flow rate elaborated. As shown in figure 6, the higher the condensation temperature, the higher the inlet vapor quality, which does not exploit any appreciable dependency from the piston displacement and thus, to the mass flow rate. As described before, fifteen T-type thermocouples have been embedded in the wall of the cold plate to monitor the wall temperature distribution during the evaporation process. The maximum wall temperature has been kept equal to 70 °C for all the investigated operation test conditions.

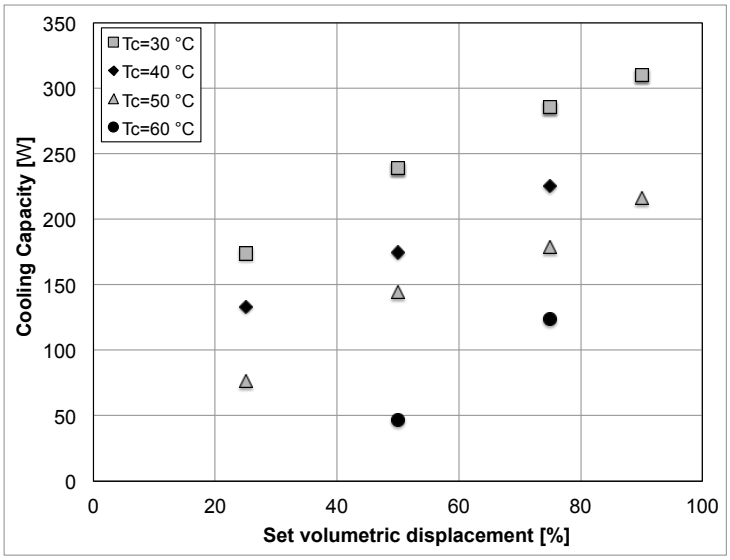

Figure 4: Cooling capacity plotted against the piston displacement as a function of the condensation temperature. Data collected at constant suction pressure of 0.49 MPa (T_{sat}=15 °C).

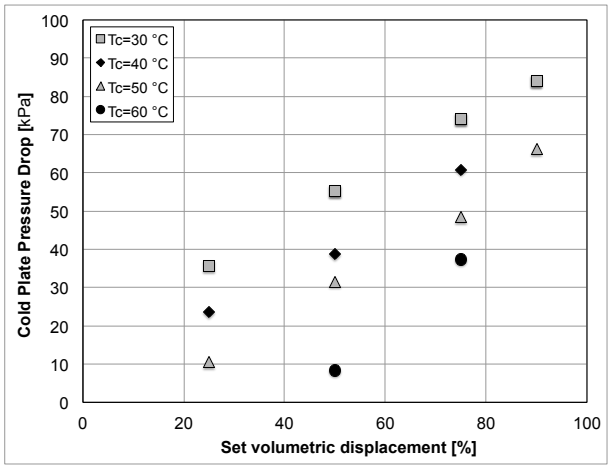

Figure 5: Cold plate refrigerant pressure drop plotted against the piston displacement as a function of the condensation temperature. Data collected at constant suction pressure of 0.49 MPa (T_{sat}=15 °C).

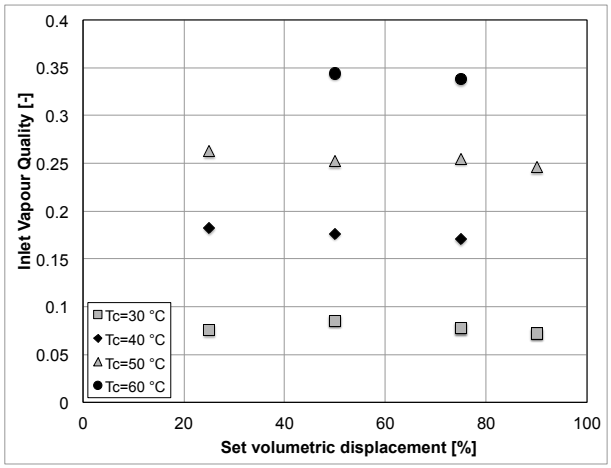

Figure 6: Inlet vapor quality plotted against the piston displacement as a function of the condensation temperature. Data collected at constant suction temperature of 0.49 MPa (T_{sat}=15 °C).

Figure 7 reports the effects of the condensation temperature on the wall temperature distribution at constant piston displacement of 50%. At 30, 40, and 50 °C, the temperature presents a plateau in the first part of the cold plate and then, it increases almost linearly up to 70 °C. It can be noticed that the length where the temperature starts to rise depends from the condensation temperature; in particular, at Tc=30 °C and Tc=40 °C the temperature can be considered constant for the first 150 mm of the cold plate. When increasing the condensation temperature from 40 °C to 50 °C, the position shifts to the left leading to a length of 125 mm.

This behavior is related to the onset of dryout during the vaporization process. In fact, the wall temperature sharply increases when the two phase heat transfer coefficient drastically falls down due to the dry out of the surface.

We can state that, from the present results, the onset dry out is delayed by the decreasing of the condensation temperature because, as shown in figure 6, the inlet vapor quality decreases as the condensation temperature decreases. Furthermore, at Tc=30 °C the first thermocouple measured around 26.5 °C while, at 40 °C and 50 °C, the measurements were around 24 °C. This can be explained considering the cold pate refrigerant pressure drop reported in Figure 5. At constant piston displacement, the pressure drop increases as the condensation temperature decreases because the refrigerant mass flow rate increases and the vapor quality simultaneously decreases (Figure 6) leading to

somewhat higher pressure drop. Therefore, since the suction temperature was kept constant at around 0.49 MPa, the pressure at the inlet of the cold plate (i.e. the saturation temperature) increases as the refrigerant pressure drop increases and, of course, the wall temperature rises up.
At Tc=60 °C, the wall temperature monotonically increases from the left side to the right side of the cold plate. This behavior can be explained considering that the inlet vapor quality was around 0.35 (figure 6) and the refrigerant mass flow rate very low being around 1.4 kg h^{-1}. In these conditions, the critical value of the vapor quality for the onset dryout is suddenly reached in the initial part of the cold plate and the temperature profile does not exhibit any plateau.

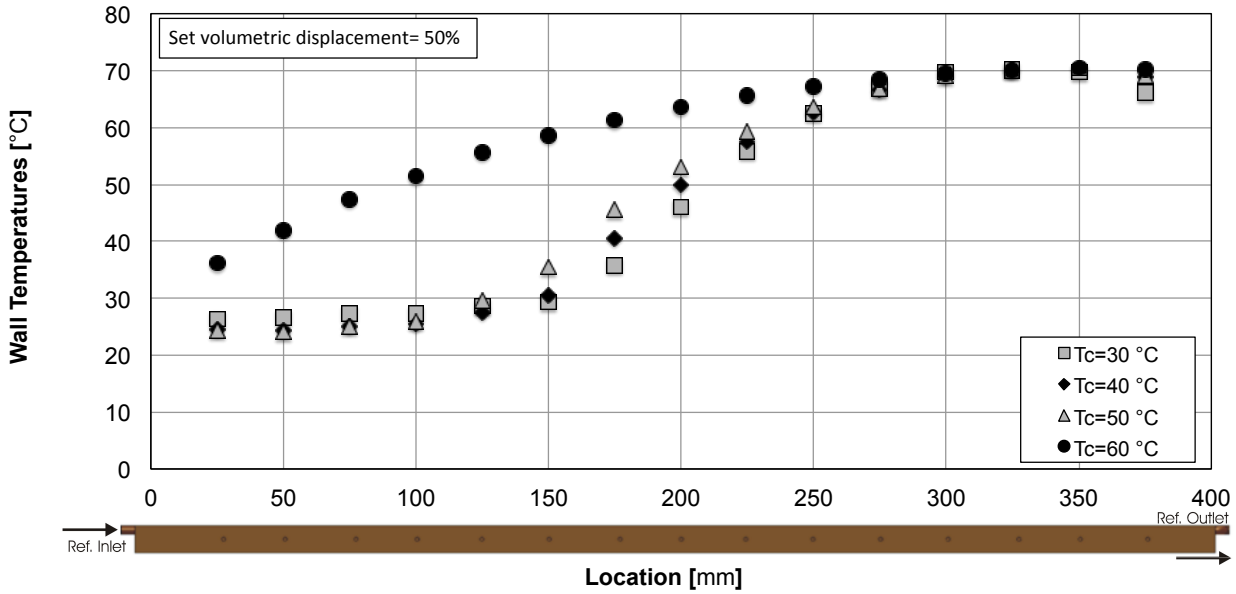

Figure 7: Wall temperature distribution at 50% of piston displacement as a function of the condensation temperature. Data collected at constant suction pressure of 0.490 MPa (T_{sat}=15 °C).

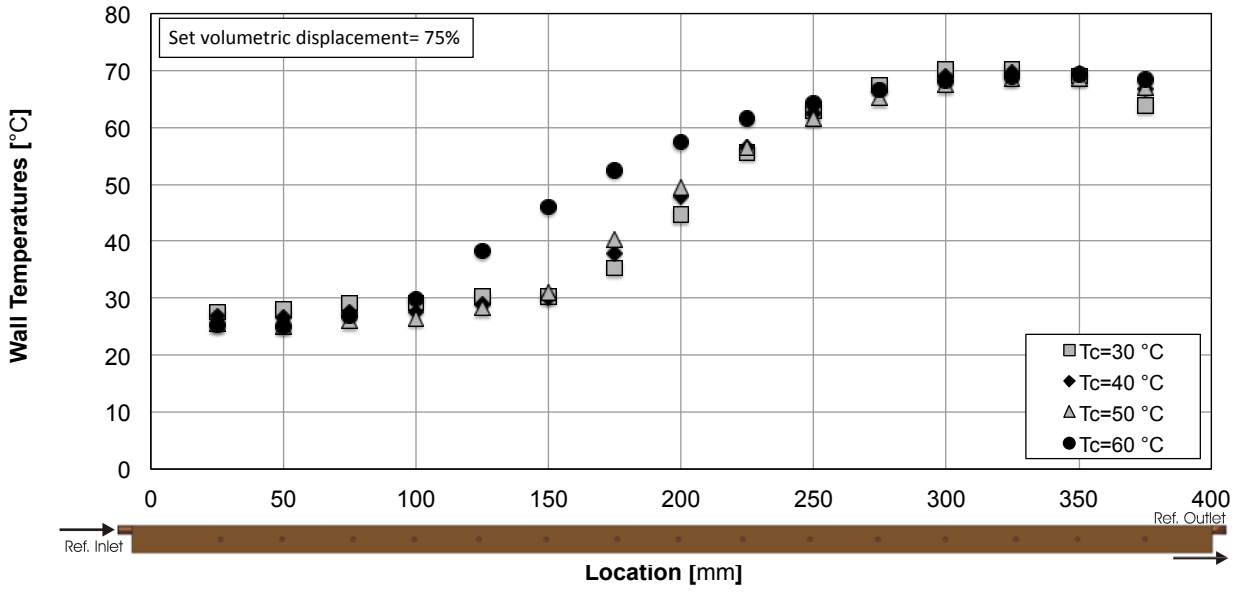

Figure 8: Wall temperature distribution at 75% of piston displacement as a function of the condensation temperature. Data collected at constant suction pressure of 0.490 MPa (T_{sat}=15 °C).

Figure 8 show the temperature profiles recorded at different condensation temperatures at constant piston displacement of 75%. At 30, 40, and 50 °C of condensation temperature, the results are similar to those highlighted before; again there is a length of the cold plate where the temperature can be considered almost constant but in this case it does not change (150 mm) as the condensation temperature increases being around 150 mm.
The difference between the behavior at 50 % and 75% of piston displacement regards the temperature distribution along the plate at Tc=60 °C: the temperature profile displays a non-negligible plateau that finishes at around 100 mm from the left side. This can be explained considering that the refrigerant mass flow rate varies from 1.3 to 2.8 kg h^{-1} when the piston displacement passes from 50% to 75% leading to a higher value of critical vapor quality for the onset dry out.

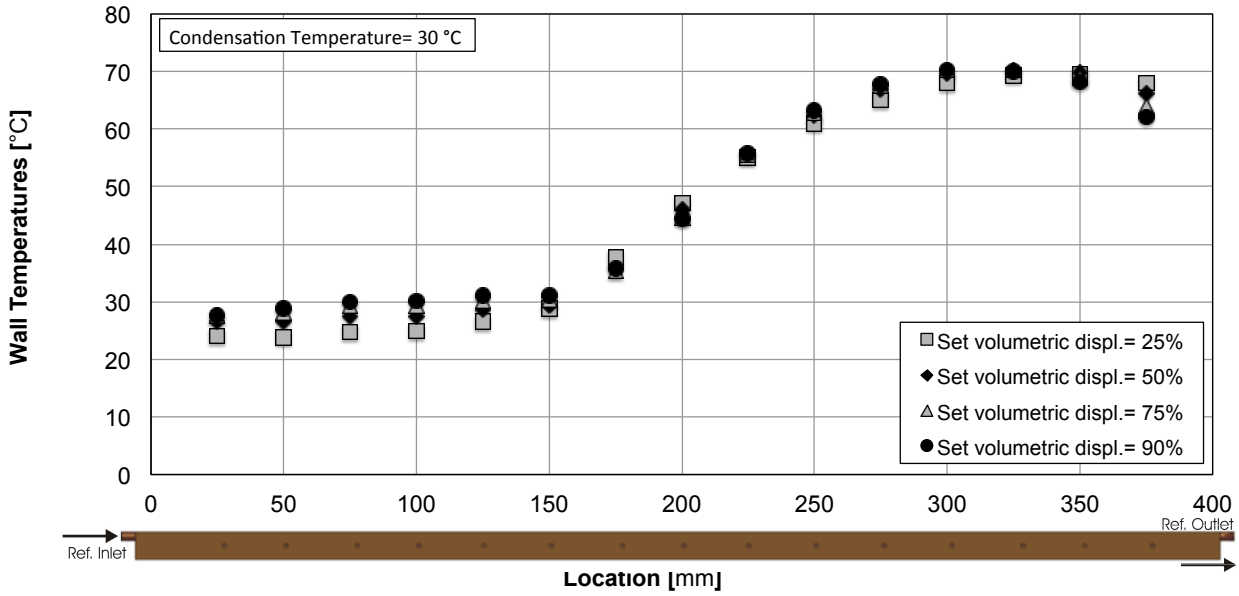

Figure 9: Wall temperature distribution at Tc=30 °C as a function of the piston displacement. Data collected at constant suction pressure of 0.490 MPa (T_{sat}=15 °C).

The effects of the piston displacement on the wall temperature distribution at constant condensation temperature are shown in Figure 9. The piston displacement was varied from 25% to 90%. As highlighted in figure 6, at Tc= 30 °C, the vapor quality at the inlet of the cold plate is almost constant being around 0.07.
The length in which the temperature can be considered constant seems to be similar for all the investigated operating test conditions and it is around 150 mm. This means that the piston displacement does not affect the dryout position; in particular, as the piston displacement increases the cooling capacity also increases and thus, since the inlet vapor quality and the outlet conditions (temperature and pressure) are almost constant, the mass flow rate also increases on the same amount. Therefore, the increasing of the heat flux imposed by the electrical heater is compensated by the higher mass flow rate, which has to be vaporized.
This means that the critical values of vapor quality for the onset dryout are reached around the same position and thus, they present also similar values.
At the inlet of the cold plate, it is evident an effect of the piston displacement on the wall temperature, since it increases as the piston displacement increases. This can be explained considering the refrigerant pressure drop reported in figure 5. As the piston displacement increases, at constant Tc= 30 °C, the refrigerant mass flow rate increases and consequently the refrigerant pressure drop during the vaporization process inside the cold also increases. Therefore, since the suction pressure is constant, the pressure at the inlet of the evaporator (i.e. the saturation temperature of the refrigerant) increases when increasing the piston displacement and, thus, the wall temperature becomes higher.
At 90% piston displacement the saturation temperature at the inlet of the cold plate is 20 °C and the first thermocouple measured a wall temperature of around 28.7 °C, while at 25%, the saturation temperature is 16.9 °C and the measured value of the wall temperature is 24.1 °C.

6. CONCLUSIONS

This paper presents the early experimental analysis of the performance of a small-scale refrigeration system within a research project aiming at investigating the suitability of miniature refrigeration systems for electronic thermal management of aeronautical packaging. Particular attention was devoted to the cold plate design, which has to comply the aeronautical volume constraints. The mini-Vapor Cycle System implements a new concept oil-free linear DC compressor prototype with variable piston displacement. The experimental measurements were carried out at constant suction pressure of 0.49 MPa that corresponds to a saturation temperature of 15 °C and four different condensation temperatures were investigated: 30, 40, 50, and 60 °C. The maximum wall temperature was set to 70 °C. In this range of operating test conditions, the cooling capacity of the system varied from 46 to 310 W and the COP ranged between 1.05 and 5.54. The analysis of the wall temperature distribution of the cold plate have highlighted the effects of the condensation temperature (i.e. inlet vapor quality) and of the piston displacement (i.e. refrigerant mass flow rate) on the heat transfer performance of the cold plate and on the vaporization process. The suitability of this mini-VCS for electronic thermal management of high density aeronautical packaging is currently under scrutiny within the research project consortium.

NOMENCLATURE

COP	Coefficient of Performance	(–)
p	Pressure	(Pa)
P_{comp}	Compressor Power	(W)
p_{dis}	Discharge Pressure	(–)
P_{EL}	Electrical Power	(W)
p_{dis}	Discharge Pressure	(Pa)
p_R	Pressure Ratio	(–)
p_{suc}	Suction Pressure	(Pa)
T	Temperature	(°C)
Tc	Condensation Temperature	(°C)
T_{sat}	Saturation Temperature	(°C)

REFERENCES

Arinc 600, 2006, Air Transport Avionics Equipment Interfaces, Specification 600-16, Aeronautical Radio Inc. Annapolis, MD, USA.

Barbosa Jr, J.R., Ribeiro G.B., de Oliveira P.A., 2012, A state-of-the-art review of compact vapor compression refrigeration systems and their applications, *Heat Transfer Engineering*, vol 33: p. 356-374.

Ribeiro G.B., 2012, Development of a high ambient temperature cooling unit based on microcompressor technology, *International Refrigeration and Air Conditioning Conference at Purdue*, July 16-19, 2012.

Kandlikar, S., Grande, W., 2004, Evaluation of single phase flow in microchannels for high flux chip cooling – Thermodynamic performance enhancement and fabrication technology, *2nd Int. Conf. On Microchannels and Minichannels*: p. 67-76.

Webb, R., 2007, Next generation devices for electronic cooling with heat rejection to air, *J. of Heat Transfer,* vol. 127: p. 2-9.

Wei, X., Joshi, Y., Patterson, M.K., 2007, Experimental and numerical study of stacked microchannel heat sink for liquid cooling of microelectronic devices, *J. of Heat Transfer* vol. 129: p. 1432-1444.

ACKNOWLEDGEMENT

The present work has been partly funded by European Commission, FP7 through the PRIMAE Project (www. primae.org, contract n. 265413) and partly funded by University of Padova through the project CPDA107382/10.
The authors gratefully acknowledge the support of Embraco Compressors, Brazil, for the supply and the implementation of the prototype compressor in the test rig.